Breast cancer invasion is mediated by β-*N*-acetylglucosaminidase (β-NAG) and associated with a dysregulation in the secretory pathway of cancer cells

K. T. RAMESSUR*, P. GREENWELL†, R. NASH‡ and M. V. DWEK*

*Departments of *Molecular and Applied Biosciences, and †Biomedical Sciences, University of Westminster, London W1W 6UW; and ‡Summit (Wales), IBERS, Plas Gogerddan, Aberystwyth, Ceredigion SY23 3EB*

Introduction

The degradation of the extracellular matrix (ECM) by proteases is an essential step in cellular invasion and cancer metastasis. Preclinical studies have shown that metastasis can be delayed by treatment of cells with protease inhibitors, but recent clinical trials with inhibitors of this type have been disappointing and have resulted in renewed interest in the identification of other enzymes important in cancer cell invasion.[1]

As the ECM is enriched with carbohydrate polymers and structural proteins it was hypothesised that glycosidases play a functional role – in concert with proteases – in mediating ECM degradation. It is presumed that the glycosidases first trim away the carbohydrate residues of the ECM to reveal the protein backbone, thereby allowing degradation by proteases, resulting in the physical space needed for cellular movement.

Most studies that relate glycosidase activity to cancer cell behaviour have focused on the endoglycosidases heparanase and hyaluronidase, which cleave within the polysaccharide chain and have been shown to mediate cancer cell invasion.[2,3] Another class of hydrolases (exoglycosidases) are found within the secretory and degradatory pathway of eukaryotic cells. These hydrolytic enzymes are normally resident in the lysosomes, endoplasmic reticulum (ER) and Golgi apparatus.[4] Lysosomal glycosidases function at an acidic pH and are involved in the degradation of macromolecules, whereas the membrane-bound glycosidases of the ER and Golgi apparatus function at a neutral pH and are glycoprotein processing or trimming enzymes.[5]

Studies have consistently shown changes in exoglycosidase activity in breast, colorectal, gastric, thyroid and ovarian cancer tissues[6–8] compared with normal tissues from the same organs. Few studies have been undertaken

Correspondence to: Dr. Miriam V. Dwek
Email: m.v.dwek@westminster.ac.uk

ABSTRACT

The extracellular matrix is enriched with carbohydrate polymers that mask the protein backbone. This study aims to test the hypothesis that for successful cancer cell invasion the cells must secrete glycosidases to reveal the protein backbone, and then the action of proteases provides the physical space needed for cancer cell movement. Thus, the activity of intracellular and secreted β-*N*-acetylglucosaminidase (β-NAG) was assayed in luminal breast epithelial cells (HB4a) and breast cancer cells (BT474, ZR75-1, MDA-MB-435, MCF7). An increase in the V_{max} of β-NAG was observed in MDA-MB-435 and MCF7 cells. Exoglycosidases are normally located in the lysosomes and function at an acidic pH, but in the cancer cells there was significant enzyme activity at neutral pH. A change in lysosome location and number was observed in the cancer cells, consistent with alterations in the secretory pathway. Finally, applying a cocktail of protease inhibitors resulted in a 20% reduction in invasion of MDA-MB-435 cells through Matrigel after 24 h, and when the cells were treated with protease and β-NAG inhibitors then cellular invasion was reduced by >60%. The results suggest combination therapies that inhibit proteases and glycosidases might be a rational way forward for the design of drugs aimed at arresting cellular invasion.

KEY WORDS: Glycoside hydrolases.
            Lysosomes.
            Matrigel.
            Neoplasm invasion.
            Neoplasms.
            Peptide hydrolases.
            Secretory pathway.
            Steviamine.

that relate exoglycosidase activity and cancer cell behaviour. The most notable work was reported nearly two decades ago and used an ovarian cancer cell line model; here, elevated levels of β-*N*-acetylglucosaminidase (β-NAG) were reported[9] and were shown to degrade the ECM.[10] Sugar analogues were found to be effective in reducing degradation of the ECM by ovarian cancer cells.[11] Recently, inhibitor molecules with greater potency have been extracted and synthesised.[12,13] Therefore, the role of glycosidases in cancer cell metastasis remains an under-researched area of biology and well-characterised models are required to enable rigorous studies in this field to be conducted.

This study systematically investigates the activity of a range of glycosidases in cell lines derived from luminal breast epithelial cells (HB4a), primary breast tumour tissue (BT474, ZR75-1) and metastatic tumour cells (MDA-MB-435, MCF7) using monosaccharide-paranitrophenol substrates. A significant increase in β-NAG was noted in MDA-MB-435 and MCF7 cells and the levels were consistent with those shown previously with breast cancer tissues.

Fractionation showed that the elevated β-NAG enzyme activity in the cancer cells was due to an increase in the β-hexosaminidase A subunit. A change in lysosome location in the cancer cells accompanied increased β-NAG secretion into the medium. Protease inhibitors were able to slow MDA-MB-435 cell movement through the ECM (as assessed using a Matrigel invasion assay) and the addition of an imino sugar inhibitor of β-NAG was able to slow the process even further.

The results confirm a role for β-NAG in cancer cell invasion and support the idea that combination therapies based on inhibiting proteases and glycosidases might be a rational way forward as a means of preventing cancer cell invasion.

Materials and methods

All materials were obtained from Sigma, Poole, UK, unless otherwise stated.

Cell culture

BT474, MCF7, MDA-MB-435, ZR75-1 and HB4a were grown as described[14–18] with 10% (v/v) fetal calf serum (FCS; Cambrex, UK) and 0.1% (v/v) gentamycin. The BT474, MCF7, MDA-MB-435 and ZR75-1 cells were a gift from Dr Susan Brooks (Oxford Brookes University, UK). The HB4a cells, a gift from Professor Mike O'Hare (University College London, UK), were a cell line originally derived from luminal epithelial cells taken from a breast reduction mammoplasty patient. The HB4a cell line was selected as a model of the 'normal breast' because gene expression microarray analysis has shown that the majority of invasive breast cancers derive from a luminal epithelial cell phenotype.[19] In contrast, benign disorders of the breast have been shown to originate from basal epithelial cells. BT474 and ZR75-1 cells have been shown to possess features consistent with luminal epithelial cells.[20]

Analyses of all five cell lines were performed within 10 passages in order to minimise the selection of fast growing clones. The cells were grown to 70–80% confluence in 75 mL flasks and harvested after washing three times with 10 mL phosphate-buffered saline (PBS) followed by incubation with 0.5 % (w/v) trypsin and 0.2% (w/v) EDTA to lift the monolayers from the plastic surface. The cells were centrifuged at 400 xg for 5 min, the supernatant was removed and cell pellets were resuspended in 1 mL PBS. A cell suspension (100 µL) was mixed with 100 µL 0.2 % (v/v) trypan blue (Cambrex, UK) and a cell count was performed using a haemocytometer. The cells were only used in the glycosidase assay if the trypan blue test showed >90% viable cells. Then, 3.8–4.2x10^6 cells were centrifuged at 400 xg for a further 5 min and the remaining PBS supernatent was decanted and the cell pellets stored at –80˚C to await cell lysis and glycosidase assay.
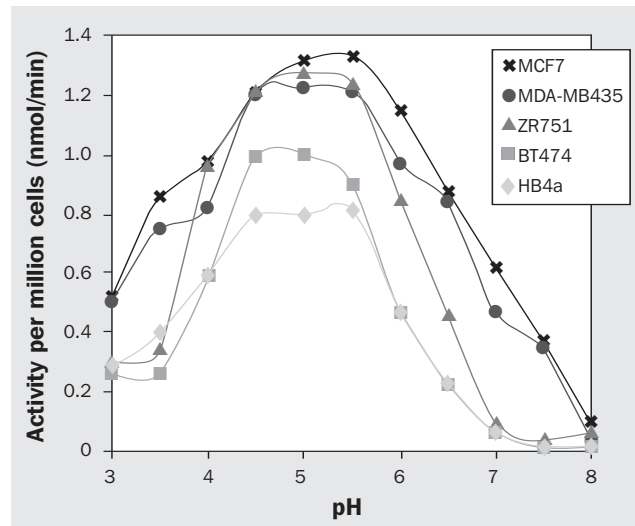
Fig. 1. β-NAG activity at different pH using cell lysate preparations from cell lines derived from primary breast cancer BT474 (square), ZR75-1 (triangle), metastatic cancer MDA-MB-435 (circle) MCF7 (cross) and normal luminal breast epithelial cells HB4a (diamond). The cells were incubated with 3.3 mmol/L pNP-β-GlcNAc for 18 h at 37˚C and the absorbance read at 405 nm. The activity of β-NAG was calculated by assessing the amount of pNP substrate released per min per million cells. The β-NAG activity was greatest in the pH range 4.5–5.5 consistent with the activity of lysosomal enzyme. The cell lines derived from metastatic tumour cells (MDA-MB-435 and MCF7) exhibited significant β-NAG activity at neutral pH.

Collection of conditioned medium for glycosidase assay

The cells were cultured in 25 mL flasks at 37˚C and 5% CO_2 until approximately 75–80% confluent, washed (x3) with 5 mL PBS and the medium was replaced with 5 mL serum-free medium. The cells were grown in serum-free medium for 24 h or 48 h. A cell viability test was undertaken using trypan blue as detailed above. To check that the cells had not been adversely affected by growth in the serum-free medium, a lactate dehydrogenase assay was undertaken using either plain Dulbecco's modified Eagle's medium (DMEM) or RPMI 1640 medium as the negative control (data not shown). After 24 h or 48 h, the medium was collected, filtered through a 0.2 mm sterile filter and dialysed overnight at 4˚C against sterile distilled water. The dialysed medium was freeze-dried (Thermo Savant, UK) and stored at –80˚C until the glycosidase activity was assayed.

Preparation of cell lysate for glycosidase assay

The cell pellets were thawed, 1 mL sterile deionised water was added and the cells were mixed well to form a cell suspension. The cells were lysed using a Status 200 sonicator fitted with a 3 mm MS 73 probe. The sonicator was used at a continuous pulse frequency of 40% duty cycle with six bursts each of 10-sec duration and at 30-sec intervals. The cells were maintained at 4˚C during the cell lysis step. The cell lysate was centrifuged at 3800 xg for 10 min and the supernatant was aliquoted and stored at –80˚C until the glycosidase assay was performed.

Glycosidase assay

The cell lysate and media samples were tested for β-NAG activity using 3.3 mmol/L pNP β-NAG substrate, prepared in deionised water and using a method adapted from Kilian
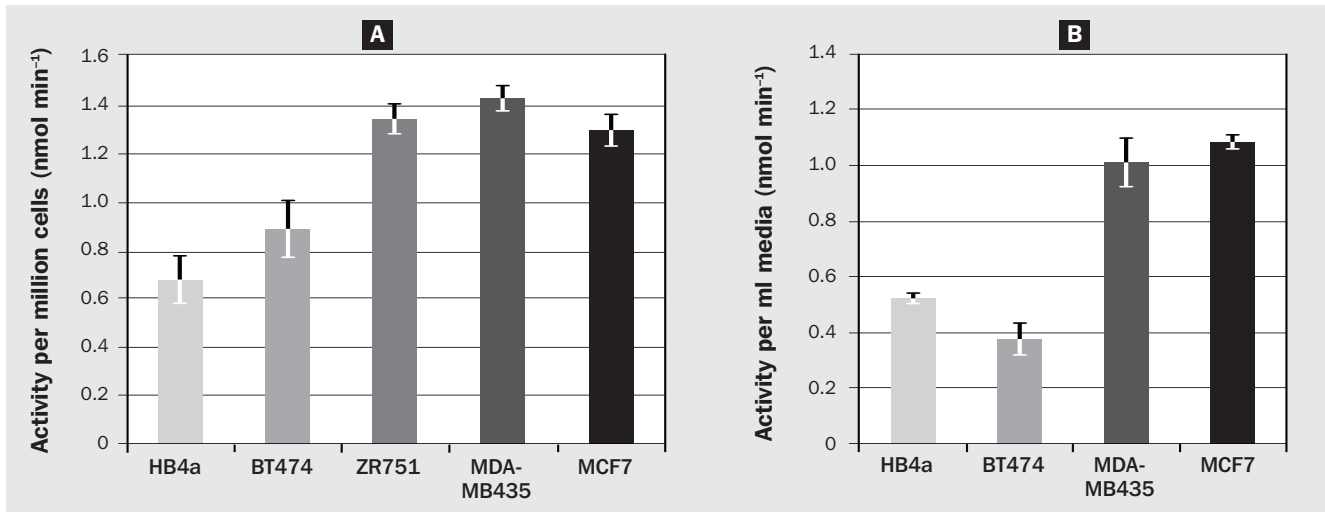
Fig. 2. β-NAG activity at pH 5.0 using cell lysate proteins (panel A) or 1 mL serum-free medium collected after 48 h (panel B). Values are mean average±standard deviation taken from three passages of cells each tested in duplicate. The cell lines derived from normal luminal breast epithelial cells (HB4a), from primary breast cancer (BT474, ZR75-1) and metastatic cancer (MDA-MB-435, MCF7) are indicated. There was significantly more β-NAG (Student's t-test, $P<0.05$) activity in ZR75-1, MDA-MB-435 and MCF7 cell lysates than for HB4a or BT474. Similarly, there was significantly more β-NAG activity (Student's t-test, $P<0.05$) in the media of MDA-MB-435 and MCF7 compared with HB4a and BT474.

and Bulow.[21] All samples (cell lysate and medium) were assayed in duplicate with three biological replicates from different cell passages. The protein content of all the samples was assayed[22] and adjusted to 0.1 mg/mL prior to use in the assay. Briefly, 25 µL protein preparation was added to 20 µL pNP-sugar in 10 µL of either 0.1 mol/L sodium citrate or 0.1 mol/L disodium hydrogen phosphate buffer. Sodium citrate buffer was used for assays between pH 3.0–6.0, while disodium hydrogen phosphate buffer was used for assays between pH 6.0–8.0. The mixture was incubated for 18 h at 37˚C and the reaction was stopped by addition of 55 µL 0.5 mol/L sodium carbonate. Colour formation was monitored by reading the absorbance at 405 nm in an MRX Dynatech plate reader. After the optimum pH for maximum activity had been determined, all subsequent experiments were undertaken at pH 5.0. The kinetics of the enzyme:substrate reaction were assessed for β-NAG at pH 5.0 and at 37˚C using a range of pNP substrate concentrations (0–12 mmol/L). The V_{max} and K_m for the enzyme:substrate interactions for the different cell lines were calculated using the Eadie-Hofstee plot.

Separation of hexosaminidase A and hexosaminidase B
All fractionation steps were undertaken at 4˚C. A 20 mL column containing DEAE-sepharose (GE Healthcare, UK) was poured, allowed to settle overnight and then washed with 10 column volumes of running buffer (50 mmol/L disodium hydrogen phosphate buffer, pH 7.0) at a flow rate of 3 mL/min. The protein preparation (2–2.5 mg/mL) was loaded onto the column in 2 mL running buffer and allowed to interact with the matrix for 45 min, and the unbound protein was washed from the column with 100 mL running buffer and collected in 10 mL fractions. Running buffer (100 mL) containing a linear gradient of sodium chloride (0.1–1 mol/L) was applied and 10 mL fractions of bound proteins were collected. The fractions were freeze-dried. Each fraction was reconstituted in 1 mL sterile distilled water and dialysed overnight against sterile high-performance

liquid chromatography (HPLC) water. The samples were stored at –80˚C until use.

mRNA extraction, reverse transcription and PCR
The expression levels of messenger RNA (mRNA) for *hexosaminidase A* (GenBank ID 3073), *hexosaminidase B* (GenBank ID 3074), *hyaluronidase 1* (GenBank ID 3373), *hyaluronidase 2* (GenBank ID 15587), *heparanase 1* (GenBank ID 10855), *cathepsin D* (GenBank ID 1509), *MMP2* (GenBank ID 4313) and *MMP9* (GenBank ID 4318) were assessed in the MDA-MB-435 cells using the polymerase chain reaction (PCR). Two batches of cells were used and the PCR reactions were undertaken in triplicate. Briefly, approximately 1×10^4 cells were taken and used for mRNA with the RNeasy Mini extraction kit (Qiagen, UK), and the purity and concentration of the mRNA was determined by measuring the ratio of absorbance at 260 nm and 280 nm in a spectrophotometer (Eppendorf, UK). The integrity of the mRNA was assessed by taking 5–10 µg extract, separating on a 2% agarose gel, staining with ethidium bromide and visualising under ultraviolet (UV) light (data not shown). Then, 1 µg mRNA was reverse transcribed to complementary DNA (cDNA) using the Quantitect reverse transcriptase kit (Qiagen, UK), and 1 ng cDNA was then amplified (in triplicate for each batch of cells) by PCR. A SYBR green PCR kit (Qiagen, UK) and a real-time cycler (ABI-Prism 7000, Applied Biosystems, UK) were used for this purpose. The initial PCR activation step was undertaken for 5 min at 95˚C, followed by a denaturation step for 10 sec at 95˚C with 35–40 annealing cycles of 30 sec at 60˚C. The primers (Qiagen, Germany) used in the PCR experiments were *hexosaminidase A*: QT00079877, *hexosaminidase B*: QT00012054, *hyaluronidase 1*: QT01673413, *hyaluronidase 2*: QT00013363, *heparanase*: QT00009555, *cathepsin D*: QT00020391, *MMP2*: QT00088396, *MMP9*: QT00040040 and *β-actin*: QT01680476. The cycle threshold (Ct) value for product formation was determined using the ABI-Prism 7000 software (using the preset parameters) and the
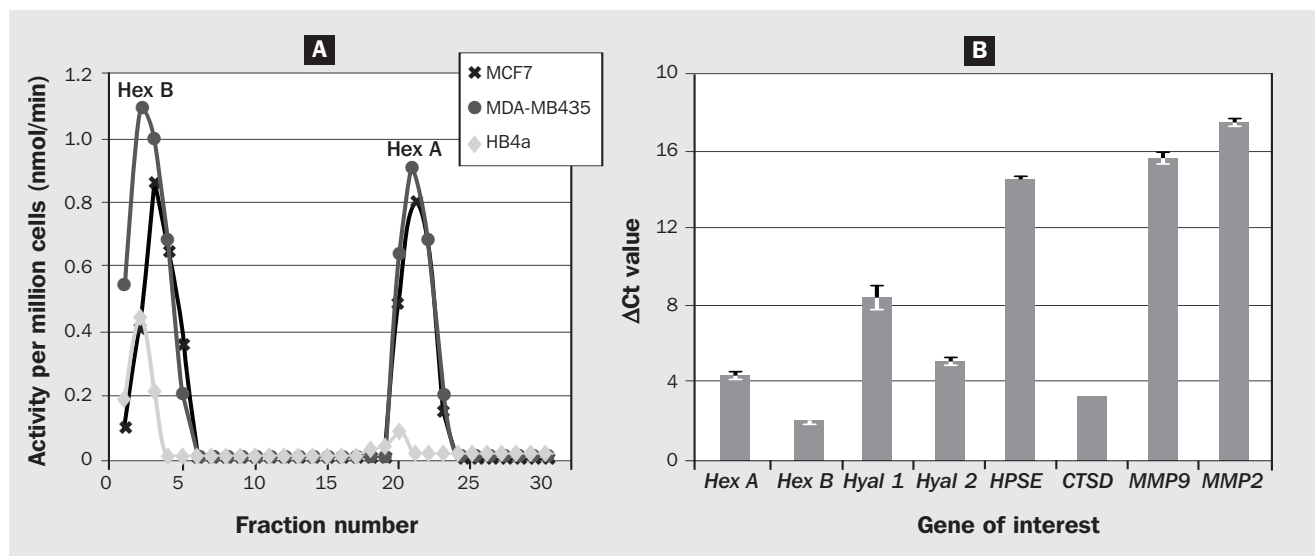
Fig. 3. Fractionation of β-NAG collected from cell lysate preparations of HB4a, MDA-MB-435 and MCF7 using anion-exchange chromatography on DEAE-sepharose resin (panel A). The β-hexosaminidase B subunit (Hex B) was collected in the unbound fraction, while the β-hexosaminidase A subunit (Hex A) was eluted with NaCl, as described in materials and methods. The cell lysate preparations from MDA-MB-435 and MCF7 contained considerably more Hex A than HB4a. The mRNA expression of *Hex A, Hex B*, hyaluronidase 1 (*Hyal1*), *Hyal2*, heparanase (*HPSE*), cathepsin D (*CTSD*), matrix metalloproteinase 9 (*MMP9*) and *MMP2* in MDA-MB-435 cells was assessed using semiquantitative RT-PCR (panel B). The cycle threshold (Ct) value for the amplification of the product was compared with *β-actin* (reference gene, data not shown). *Hex B, CTSD, Hyal2* and *Hex A* were found in the greatest amounts with minimal expression of *HPSE, MMP2* and *MMP9* observed. The results are mean average values±standard error of two biological experiments, each evaluated in triplicate.

expression level of the gene of interest was then compared to the Ct value for a reference gene (*β-actin*) run at the same time giving values for the change in Ct (ΔCT). The PCR products were separated by electrophoresis as before to confirm the length of the amplicons (data not shown).

Confocal microscopy with the Lysotracker dye DND99
The HB4a, MDA MB 435 and MCF 7 cells (2.5×10^5) were seeded in individual six-well plates and grown as before until approximately 75% confluent. The cells were washed with appropriate plain medium and incubated with 0.1 mol/L ribonuclease A for 20 min at 37°C. The six-well plates were maintained in the dark for the remainder of the staining process. The cells were washed in plain medium and incubated with 100 nmol/L/mL Lysotracker DND99 dye (Invitrogen, UK) for 60 min at 37°C, washed three times with plain medium and the nuclei counterstained with 30 ng/mL acridine orange (Invitrogen, UK) for 5 min at 37°C. The cells were washed as before and examined under a Leica TCS SP2 confocal microscope (Leica Microsystems, Milton Keynes, UK) using a ceramic dipping objective (x63 magnification), a 1024x1024 pixel format, a scanning speed of 400 Hz and a line average of 8. The pinhole aperture was set to 1 Airy unit. A 488 nm laser (intensity: 25%) was used for the excitation of acridine orange and a 543 nm laser (intensity: 73%) was used for the Lysotracker DND99 dye. Emission spectra were recorded using a bandwidth of 500–535 nm for acridine orange and 560–623 nm for the Lysotracker dye. The background was compensated by adjusting the gain and offset commands. Two-dimensional (2D) models and lysosomal counts were performed using the Imaris Surpass tool (Bitplane, Germany). After baseline correction, lysosome number was determined by counting cellular structures >0.4 μm in diameter that took up the Lysotracker dye. For each cell line, eight to 10 fields were

taken and used to obtain an average reading for the lysosome number per cell line.

Glycosidase and protease inhibition
The MDA-MB-435 cells were seeded into selected wells of a 24-well plate grown to near-confluence in DMEM with 10% FCS. The cells were washed (x3) with 0.2 mL PBS and incubated with the imino sugar steviamine (Summit, UK)[23] prepared in DMEM. The effect of varying incubation time (24 h and 48 h) and inhibitor concentration (0.25 mmol/L, 0.5 mmol/L and 1 mmol/L) on cell movement through a scratched surface of the monolayer and on cell viability was assessed and compared to cells grown in DMEM (data not shown). After the incubation period, the medium was collected, centrifuged at 3800 x*g* at 4°C for 2 min to pellet any cells that had detached from the monolayer, and the supernatant was dialysed overnight at 4°C against sterile deionised water. The cells in the wells were washed (x3) with PBS, harvested and lysed as before. A protein assay was performed using the samples of medium and the cell lysate, and β-NAG was assayed using the method above. A cocktail

Table 1. V_{max} and K_m values for β-NAG from cell lysate preparations of the cells used in this study.

Cell line	V_{max} (nmol per min/10^6 cells)	K_m (mmol)
HB4a	0.79	1.75
BT474	0.89	1.79
ZR75-1	1.56	1.89
MDA-MB-435	1.73	1.92
MCF7	1.85	2.10
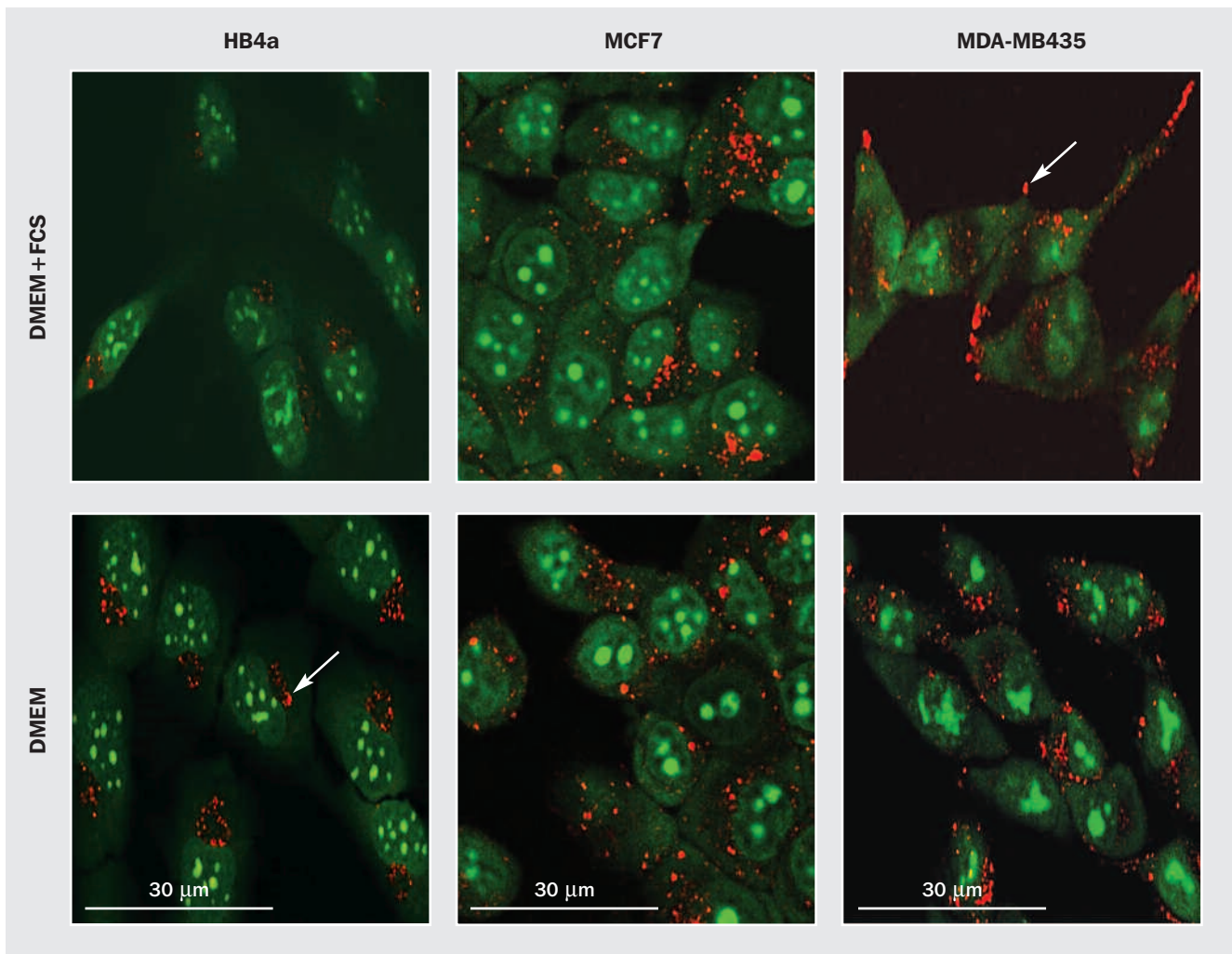
Fig. 4. Lysosome staining with Lysotracker dye (red) of cells derived from normal luminal breast epithelium (HB4a) and metastatic cancer (MDA-MB-435, MCF7). The nuclei were counterstained using acridine orange (green). Cells were grown for 48 h in either DMEM supplemented with 10% v/v fetal calf serum (DMEM+FCS) or in serum-free medium (DMEM) prior to staining. The lysosome number was increased in all three cell lines when they were grown for 48 h in DMEM without FCS. The MCF7 cells exhibited disordered lysosomal distribution and in MDA-MB-435 the lysosomes were observed in the filipodia (arrows). In contrast, for HB4a the lysosomes were confined to the perinuclear region. The cells were visualised using a Leica TCS SP2 microscope system fitted with dipping objective (x63 magnification).

of protease inhibitors was used, either alone or in conjunction with the imino sugar inhibitor. The protease inhibitor cocktail contained 200 µmol/L 2-aminoethyl benzenesulphonyl fluoride (AEBSF), 100 µmol/L EDTA, 13 µmol/L bestatin, 1.4 µmol/L L-trans-epoxysuccinyl-leucylamide-4-guanido-butane (E-64), 0.1 µmol/L leuceptin and 0.03 µmol/L aprotinin and was diluted (1 in 1000) in DMEM. To exclude the possibility that protease inhibitors may cause changes in glycosidase level, the cells were incubated with the protease inhibitors and the activity of β-NAG was assessed as before. The cell viability assay using trypan blue showed that >90% of cells remained intact after treatment with protease and glycosidase inhibitors.

Matrigel invasion assay
Matrigel invasion chambers with 8 µm membrane pore size and in 24-well plate format were used (BD Biosciences, UK). The cell culture inserts were thawed and 0.5 mL warm, plain DMEM medium was added to the interior of the insert and the bottom of the companion plate. The insert was

rehydrated for 2 h in a humidified tissue culture incubator at 37°C and 5% CO_2. The medium was removed carefully from the surface of the insert. A chemoattractant (DMEM containing 10 % [v/v] FCS) was added to the lower well of the companion plate. The MDA-MB 435 cells were prepared ($5.0–8.0 \times 10^4$ cells/mL) in 500 µL either plain DMEM or medium containing protease inhibitor cocktail or medium containing protease inhibitor and 1 mmol/L imino sugar glycosidase inhibitor. The cells were added to the hydrated inserts and incubated for 24 h, the supernatant was removed and a cell viability assay was performed. The non-invading cells and the Matrigel matrix were removed from the upper surface of the membrane with a cotton swab moistened with DMEM. The process was repeated with a second moist swab until no cells remained attached to the upper surface of the membrane. The upper surface was washed (x3) with PBS. The lower surface of the membrane was soaked in 1 ml PBS containing trypsin-EDTA and incubated at 37°C for 5 min to detach any adherent cells. The cells recovered from the membrane were centrifuged at 3800 x*g* for 2 min. The

Fig. 5. The activity of β-NAG in 100-μL medium from MDA-MB-435 cells after incubation for 24 h with DMEM (light grey bar), DMEM supplemented with a cocktail of protease inhibitors (mid-grey bar) or DMEM supplemented with protease inhibitors and 1 mmol/L imino sugar glycosidase inhibitor (black bar). A significant reduction in β-NAG activity was observed when the glycosidase inhibitor was applied to the cells (panel A). The invasive properties of MDA-MB-435 cells were assessed in the Matrigel assay system (panel B). Cells were treated as above (for 24 h) and the number of cells that migrated through the matrix was counted. A reduction in cellular invasion was observed when the cells were treated with the cocktail of protease inhibitors, and a further reduction was observed when this was supplemented with the glycosidase inhibitor.
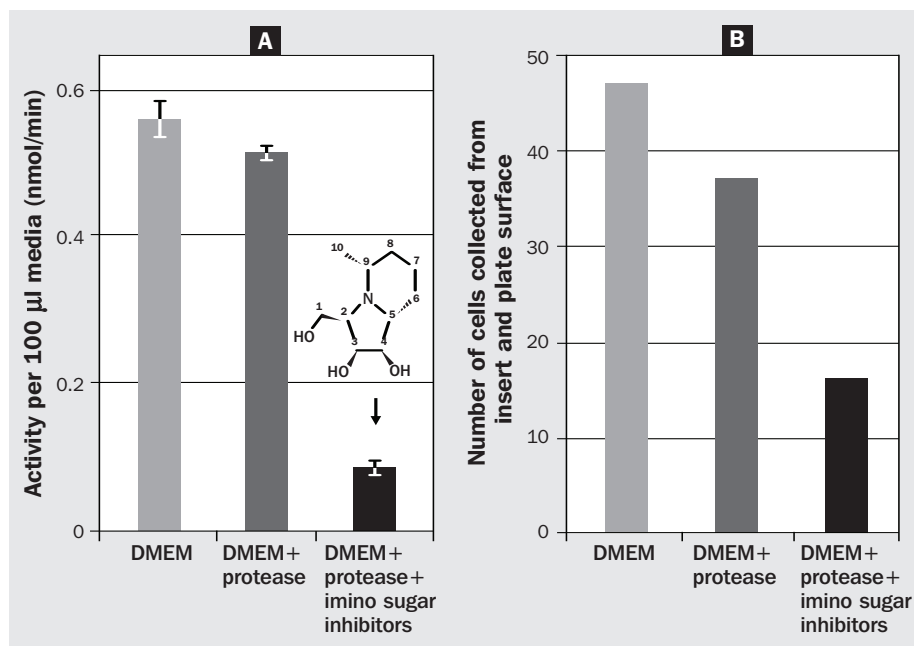
supernatant was removed and the cell pellets were resuspended in 500 μL complete DMEM medium, seeded into a new 24-well plate and a further 500 μL DMEM medium added. The 24-well plate and companion plate from the Matrigel assay were incubated for 48 h. After this second incubation step, both plates were washed (x3) with PBS and the cells were fixed for 60 min with absolute methanol. The cells were then washed further (x3) with PBS and the nuclei were stained with Harris' haematoxylin for 15 min. The excess haematoxylin dye was removed by washing in tap water and the cells were examined with a Zeiss Axiovert S100 inverted microscope using a x40 objective. The total number of cells in all the wells was counted.

Statistical analysis
The results were compared using Student's *t*-test (paired) and significant difference was taken as $P \leq 0.05$.

Results

Optimum pH for maximal β-NAG activity
The cells all showed maximum β-NAG activity in the pH range 4.5–5.5 (Fig. 1). Rather surprisingly, the two metastatic cancer cell lines (MDA-MB-435 and MCF7) also showed activity at neutral pH, a feature that was not observed in the cell lines derived from the normal luminal breast epithelium (HB4a) or primary cancer (BT474, ZR75-1).

Enzyme activity in HB4a, BT474, ZR75-1, MDA-MB-435 and MCF7 cancer cell lines
The cancer cells ZR75-1, MDA-MB-435 and MCF7 showed significant elevation in β-NAG activity compared with HB4a cells (Fig. 2, panel A). This was accompanied by a greater than two-fold increase in V_{max} (Table 1). The K_m was very similar for all cell lines. Media from MDA-MB-435 and MCF7 also showed significantly increased β-NAG activity compared to the media from HB4a and BT474 (Fig. 2, panel B).

Fractionation of hexosaminidase subunits and glycosidase/protease expression levels
The kinetic data coupled with the results for enzyme activity at different pH suggested that isoenzymes, or different enzymes exhibiting shared substrate specificities, were present in the cancer cells. To investigate this, cell lysate preparations from the MDA-MB-435, MCF7 and HB4a cells were fractionated using anion-exchange chromatography (Fig. 3, panel A). Using this approach, a near equal ratio was observed of Hex B:Hex A subunits in the medium from MDA-MB-435 and MCF7; however, when the medium from HB4a was evaluated the results showed a considerably higher Hex B:Hex A ratio. The PCR results broadly supported the enzymatic data, with MDA-MB-435 cells exhibiting the highest expression levels of *Hex B*, *Hex A* and *hyaluronidase* 2; however, while *hyaluronidase 1*, *heparanase*, *cathepsin D*, *MMP*2 and *MMP*9 were detectable (Fig. 3, panel B) they were found in considerably lower levels.

Lysosome numbers and localisation
To address the possibility that the increased activity of hexosaminidase in the media of MDA-MB-435 and MCF7 was due to a change in lysosome size, number or intracellular location, a study was undertaken using a fluorescent lysosomal tracker dye (Lysotracker DND99; Fig. 4). The staining was more intense for the two cancer cell lines compared with HB4a, irrespective of growth conditions. The cancer cells displayed a scattered staining pattern compared to the perinuclear staining observed in HB4a. In MDA-MB-435, the filipodia stained strongly with the Lysotracker dye, suggesting that the lysosomes are mainly located in the tips of these cells. A three-fold increase in lysosome number was recorded for MDA-MB-435 and MCF7 cells grown in DMEM with 10% FCS, compared with HB4a. The number of lysosomes increased when the cells were grown under serum-free conditions. Nevertheless, even in serum-free medium, the cancer cells exhibited twice the number of lysosomes compared with HB4a. Taken together, the data are consistent with a dysregulation of the secretory pathway in the cancer cells.

Invasion assay and inhibition of glycosidases/proteases
The cells were grown in the presence of a cocktail of protease inhibitors with or without supplementation with 1 mmol/L imino sugar inhibitor. As expected, the combined protease inhibitor and glycosidase inhibitor treatment decreased β-NAG activity, while the protease inhibitors (used alone) had no significant effect on enzyme activity (Fig. 5, panel A). About 20% fewer MDA-MB-435 cells migrated through the ECM when the cells were treated with the cocktail of protease inhibitors (Fig. 5, panel B) compared with cells prepared in DMEM alone. On feeding the cells with both protease and glycosidase inhibitors (in combination), 64% fewer cells moved through the ECM material compared with cells prepared in DMEM alone. In this experiment (using both glycosidase and protease inhibitors) a reduction was observed in cell migration through Matrigel compared to when the cocktail of protease inhibitors was used alone, and there appeared to be a synergistic effect when the two groups of inhibitors were used together.

Discussion

This study validated a model for cancer cell migration based on established cell lines collected at different stages of breast cancer progression. In this system, a significant increase (*P*<0.05) in β-NAG activity was observed in the cancer cell lines (MCF7, MDA-MB-435, ZR 751 and BT 474) compared to the normal breast cell line (HB4a). These data support earlier reports using breast cancer tissue samples.[6,24] The kinetic analysis showed a two-fold increase in the V_{max} of β-NAG in the cancer cell lysate, although the underlying cause of this increased activity remains unclear.

β-NAG was measured in the media of MDA-MB-435 and MCF7 cancer cells and was found in higher levels than in HB4a. Treatment of MDA-MB-435 cells with glycosidase and protease inhibitors resulted in a significant decrease in secreted β-NAG activity and a 60–70% decrease in invasion of cancer cells through Matrigel material. The study provides strong evidence that secreted β-NAG facilitates invasion of MDA-MB-435 cells through the basement membrane.

It was observed that β-hexosaminidase A activity was higher in the cancer cell lines compared to the normal control cells, and an increase in β-hexosaminidase A has been reported in the leucocytes of leukaemia patients[25] and metastatic liver tissue.[26] It would be interesting to investigate further how elevated levels of the β-hexosaminidase A isoform relate to cancer cell migration through the ECM. It has been suggested that intracellular traffic of lysosomal proteins are dysregulated in cancer cells, either because proteins targeted to lysosomes are diverted to the secretory pathway (by exhibiting low binding affinity for the mannose-6-phosphate receptor in the Golgi apparatus) or due to a dysregulation of the intracellular lysosome traffic.[27] It would be of value to investigate further both these hypotheses using relevant fluorescent-labelled antibodies and confocal microscopy in this system.

Based on the evidence that more than 50% of human proteins are glycosylated,[28] the failure of drugs that inhibit MMPs to decrease cancer metastasis,[29,30] and the hypothesis that cell membrane glycosidases are functional in the degradation of the ECM material,[11] this study highlights the functional role of glycosidases in the degradation of the ECM in breast cancer. In this system, breast cancer cells secrete glycosidases early in the metastatic process, and the enzyme then degrades the protective cell surface glycans of the ECM and, at a later stage, proteases are secreted to degrade the polypeptide backbone, thereby facilitating breast cancer cell extravasation. Further studies are now required to expand the analysis to other cell lines and to investigate the potential of using a combination of imino sugars and protease inhibitors to inhibit cancer cell migration. □

References

1 Lah TT, Durán Alonso MB, Van Noorden CJ. Antiprotease therapy in cancer: hot or not? *Expert Opin Biol Ther* 2006; **6** (3): 257–79.

2 Roy M, Marchetti D. Cell surface heparin sulphate released by heparanase promotes melanoma cell migration and angiogenesis. *J Cell Biochem* 2009; **106** (2): 200–9.

3 Lokeshwar VB, Cerwinka WH, Lokeshwar BL. HYAL1 hyaluronidase: a molecular determinant of bladder tumor growth and invasion. *Cancer Res* 2005; **65** (6): 2243–50.

4 Henrissat B, Davies G. Structural and sequence-based classification of glycoside hydrolases. *Curr Opin Struct Biol* 1997; **7** (5): 637–44.

5 Elbein AD. Inhibitors of glycoprotein synthesis. *Methods Enzymol* 1983; **98**: 135–54

6 Bosmann HB, Hall TC. Enzyme activity in invasive tumors of human breast and colon. *Proc Natl Acad Sci USA* 1974; **71** (5): 1833–7.

7 Gil-Martin E, Gil-Seijo S, Nieto-Novoa C, Fernandez-Briera A. Elevation of acid glycosidase activities in thyroid and gastric tumors. *Int J Biochem Cell Biol* 1996; **28** (6): 651–7.

8 Gil-Martin E, Rodriguez-Berrocal J, Paez de la Cadena M, Fernandez-Briera A. Alterations of glycosidases in human colonic adenocarcinoma. *Clin Biochem* 1997; **30** (1): 17–25.

9 Niedbala MJ, Madiyalakan R, Matta K, Crickard K, Sharma M, Bernacki RJ. Role of glycosidases in human ovarian carcinoma cell mediated degradation of subendothelial extracellular matrix. *Cancer Res* 1987; **47** (17): 4634–41.

10 Woynarowska B, Skrincosky DM, Haag A, Sharma M, Matta K, Bernacki RJ. Inhibition of lectin-mediated ovarian tumor cell adhesion by sugar analogs. *J Biol Chem* 1994; **269** (36): 22797–803.

11 Woynarowska B, Wikiel H, Bernacki RJ. Human ovarian carcinoma beta-*N*-acetylglucosaminidase isoenzymes and their role in extracellular matrix degradation. *Cancer Res* 1989; **49** (20): 5598–604.

12 Wrodnigg TM, Steiner AJ, Ueberbacher BJ. Natural and synthetic iminosugars as carbohydrate processing enzyme inhibitors for cancer therapy. *Anticancer Agents Med Chem* 2008; **8** (1): 77–85.

13 Rountree JS, Butters TD, Wormald MR *et al*. Design, synthesis and biological evaluation of enantiomeric

beta-*N*-acetylhexosaminidase inhibitors LABNAc and DABNAc as potential agents against Tay-Sachs and Sandhoff disease. *Chem Med Chem* 2009; **4** (3): 378–92.

14 Lasfargues EY, Coutinho WG, Redfield ES. Isolation of two human tumor epithelial cell lines from solid breast carcinomas. *J Natl Cancer Inst* 1978; **61** (4): 967–97.

15 Engel LW, Young NA, Tralka TS, Lippman ME, O'Brien SJ, Joyce MJ. Establishment and characterization of three new continuous cell lines derived from human breast carcinomas. *Cancer Res* 1978; **38** (10): 3352–64.

16 Cailleau R, Young R, Olive M, Reeves WJ. Breast tumour cell lines from pleural effusions. *J Natl Cancer Inst* 1974; **53** (3): 661–673.

17 Soule HD, Vazquez J, Long A, Albert S, Brennan M. A human breast cancer cell line from pleural effusion derived from a breast carcinoma. *J Natl Cancer Inst* 1973; **51** (5): 1409–16.

18 Stamps AC, Davies SC, Burman J, O'Hare MJ. Analysis of proviral integration in human mammary epithelial cell lines immortalized by retroviral infection with a temperature-sensitive SV40 T-antigen construct. *Int J Cancer* 1994; **57** (6): 865–74.

19 Perou CM, Sørlie T, Eisen MB *et al*. Molecular portraits of human breast tumours. *Nature* 2000; **406** (6797): 747–52.

20 Jönsson G, Staaf J, Olsson E *et al*. High-resolution genomic profiles of breast cancer cell lines assessed by tiling BAC array comparative genomic hybridization. *Genes Chromosomes Cancer* 2007; **46** (6): 543–58.

21 Kilian M, Bulow P. Rapid diagnosis of Enterobacteriaceae I. Detection of bacterial glycosidases. *Acta Pathol Microbial Scand B* 1976; **84B** (5): 245–51.

22 Bradford MM. A rapid and sensitive method for the quantitation of microgram quantities of protein utilizing the principle of protein-dye binding. *Anal Biochem* 1976; **72**: 248–54.

23 Thompson AL, Michalik A, Nash RJ *et al*. Steviamine, a new class of indolizidine alkaloid [(1R,2S,3R,5R,8aR)-3-(Hydroxymethyl)-5-methyloctahydroindolizine-1,2-diol hydrobromide]. *Acta Crystallogr C* 2009; **E65**: o2904–5 (doi:10.1107/S1600536809043827).

24 Slawson C, Pidala J, Potter R. Increased *N*-acetyl-β-glucosaminidase activity in primary breast carcinomas corresponds to a decrease in *N*-acetyl-glucosamine containing proteins. *Biochim Biophys Acta* 2001; **1537**: 147?57.

25 Martino S, Emiliani C, Tabilio A, Falzetti F, Stirling JL, Orlacchio A. Distribution of active alpha- and beta-subunits of beta-*N*-acetylhexosaminidase as a function of leukaemic cell types. *Biochim Biophys Acta* 1997; **1335** (1–2): 5–15.

26 Alhadeff JA, Holzinger RT. Presence of an atypical thermolabile species of beta-hexosaminidase B in metastatic tumour tissue of human liver. *Biochem J* 1982; **201** (1): 95–9.

27 Dong JM, Sahagian GG. Basis for low affinity binding of a lysosomal cysteine protease to the cation-independent mannose 6-phosphate receptor. *J Biol Chem* 1990; **265** (8): 4210–7.

28 Varki A. Glycosylation changes in cancer. In: Varki A, Esko J, Cummings R, Freeze HH, Hart GW, Marth J eds. *Essentials of glycobiology*. Plainview NY: Cold Spring Harbor Laboratory Press, 1999.

29 Zucker S, Cao J, Chen WT. Critical appraisal of the use of matrix metalloproteinase inhibitors in cancer treatment. *Oncogene* 2000; **19**: 6642–50.

30 Coussens LM, Fingleton B, Matrisian LM. Matrix metalloproteinase inhibitors and cancer: trials and tribulations. *Science* 2002; **295** (5564): 2387–92.